AGARD-AR-303 Vol. II

AGARD

ADVISORY GROUP FOR AEROSPACE RESEARCH & DEVELOPMENT
7 RUE ANCELLE, 92200 NEUILLY-SUR-SEINE, FRANCE

AGARD ADVISORY REPORT NO 303

A Selection of Experimental Test Cases for the Validation of CFD Codes

(Recueil de cas d'essai expérimentaux pour la validation des codes de l'aérodynamique numérique)

Volume II

This Advisory Report was prepared at the request of the Fluid Dynamics Panel.

NORTH ATLANTIC TREATY ORGANIZATION

Published August 1994

Distribution and Availability on Back Cover

REPRODUCED BY:
DEPARTMENT OF COMMERCE
National Technical Information Service
Springfield, Virginia, 22161

The Mission of AGARD

According to its Charter, the mission of AGARD is to bring together the leading personalities of the NATO nations in the fields of science and technology relating to aerospace for the following purposes:

- Recommending effective ways for the member nations to use their research and development capabilities for the common benefit of the NATO community;
- Providing scientific and technical advice and assistance to the Military Committee in the field of aerospace research and development (with particular regard to its military application);
- Continuously stimulating advances in the aerospace sciences relevant to strengthening the common defence posture;
- Improving the co-operation among member nations in aerospace research and development;
- Exchange of scientific and technical information;
- Providing assistance to member nations for the purpose of increasing their scientific and technical potential;
- Rendering scientific and technical assistance, as requested, to other NATO bodies and to member nations in connection with research and development problems in the aerospace field.

The highest authority within AGARD is the National Delegates Board consisting of officially appointed senior representatives from each member nation. The mission of AGARD is carried out through the Panels which are composed of experts appointed by the National Delegates, the Consultant and Exchange Programme and the Aerospace Applications Studies Programme. The results of AGARD work are reported to the member nations and the NATO Authorities through the AGARD series of publications of which this is one.

Participation in AGARD activities is by invitation only and is normally limited to citizens of the NATO nations.

Published August 1994

ISBN 92-836-1003-2

Printed by Canada Communication Group
45 Sacré-Cœur Blvd., Hull (Québec), Canada K1A 0S7

DLR-F4 WING BODY CONFIGURATION

by

G. REDEKER

DEUTSCHE FORSCHUNGSANSTALT FÜR LUFT-UND RAUMFAHRT E.V. (DLR)
INSTITUT FÜR ENTWURFSAERODYNAMIK

Lilienthalplatz 7
D-38108 BRAUNSCHWEIG
GERMANY

0 INTRODUCTION

These tests have been carried out under the auspices of GARTEUR in order to provide an experimental data base for a modern commercial transport type aircraft against which results of various computational methods may be checked. The tests were carried out in three major European wind tunnels (NLR-HST, ONERA-S2MA, DRA-8ft x 8ft DRA Bedford) in order to compare the results of the same model in different wind tunnels. For the purpose of these tests the available geometry of the DLR-F4 model of a wing body configuration, which was developed as a research configuration of a modern transport type aircraft, was selected by the GARTEUR Action Group AD (AG01) 'Wing body aerodynamics at transonic speeds'.

GENERAL DESCRIPTION

1.1 Model name	DLR-F4 model [1].
1.2 Model type and flow conditions	Wing body configuration of a subsonic transport type aircraft. Attached transonic flow on swept back wing of aspect ratio 9.5.
1.3 Design requirements, purpose of tests	Transonic swept wing flow in M-range 0.75-0.8 with supersonic flow regions on upper wing surface terminated by weak shock waves. Data base for validation of 3D transonic codes. Comparison of data for the same model in different wind tunnels.
1.4 Dominant flow physics	Transonic or supercritical flow on sweptback wing with weak shock waves. A small trailing edge separation is present at design condition in the kink region of the trailing edge.

2 DETAILS OF MODEL

2.1 General geometric arrangement	Wing body combination; see Fig. 1.
2.2 Configuration tested	Wing body configuration and body alone tested
2.3 Wing and airfoil data	
2.3.1 Planform	See Fig. Aspect ratio $\Lambda = 9.5$; taper $\lambda = 0.3$ L.E. sweep $\varphi_{LE} = 27.1°$; 25% sweep $\varphi_{25} = 25°$ Twist distribution incorporated in wing sections. Semispan $s = 0.5857$ m Wing ref. area: $S = 0.1454$ m^2 Aerodynamic mean chord: $\bar{c} = 0.1412$m Tip geometry: half circle of local wing section thickness inside side edge of wing planform. No special wing/body junction; sharp corner.

2.3.2 Basic wing sections	Wing section shapes see Fig. 2. Wing built up by 4 defining sections as shown in Fig. 2.
2.4 Body data	
2.4.1 Shape	Nose and afterbody shape see Fig. 3. Body length l = 1.1920 m. Cross-sectional details see geometry data disk.
2.7 Geometric definition of c mponents	Wing: Numerically specified by 4 defining sections (Fig. 2). Wing contour is generated by linear lofting between defining sections. Body: Numerically specified by 90 cross-sections x = const. . Data are design coordinates. Tolerances: wing and body ±0.05 mm.
2.8 Model support details (DRA)	The model was mounted on an axisymmetric sting passing through a hole of elliptic cross- section in the rear of the body (Fig. 4).
2.8 Model support details (NLR)	NLR Z-sting Nr. 002 (see Fig.5 and 6); a small unsealed gap is present at the location where the blade enters the model.
2.8 Model support details (ONERA)	ONERA Z-sting see Fig. 7.

3 GENERAL TUNNEL INFORMATION (DRA)

3.1 Tunnel designation	8ft x 8ft Pressurised, Subsonic/Supersonic Wind Tunnel.
3.2 Organisation running the tunnel	Defense Research Agency (formerly Royal Aerospace Establishment), Aerodynamic and Propulsion Department, Bedford MK41 6AE, England.
3.3 Tunnel characteristics	Type of tunnel: continuous flow, closed circuit. Operating envelope see Fig. 8.
3.4 Test section	
3.4.1 Model mounting	See Fig. 4.
3.4.2 Test section dimensions	2.44 m x 2.44 m x 14 m (width x height x length).
3.4.3 Wall geometry details	Type of walls: solid, flexible upper and lower walls for supersonic operation. Shapes of upper and lower walls are set for subsonic tests in such a way as to minimise the pressure gradient on the centre line when the test section is empty. Wall pressures are measured along the centre lines of the roof and floor. Typical wall boundary-layer displacement thickness: 19 mm. For further details see [2].
3.5 Freestream conditions	
3.5.1 Reference conditions	Total pressure: Determined using a pitot probe in the settling chamber and a 'Midwood' self-balancing capsule manometer of range 400 kPa and accuracy ±0.03% full scale. Static pressure: The reference static pressure tapping is on the centre-line of the sidewall 6.25 m upstream of the strain-gauge balance centre-line. The differential 'Midwood' mano-meter used for this measurement was of range 100 kPa and accuracy 0.03% full scale. Static temperature: This is inferred from total temperature measured to an accuracy of ± 0.1K by a probe in the settling chamber.
3.5.2 Tunnel calibration	Measurements were made of static pressures on the test section centre-line and roof and floor [3] using differential 'Midwood' manometers of range ± 100kPa and accuracy ± 0.03% full scale. The last calibration was performed (using electronic scanning of pressure transducers) in October 1991, calibrations being performed annually.

3.6 Flow quality

3.6.1 Flow uniformity	For static pressure variations along the model axis see [3], but typically $\Delta c_p < 0.001$ with the diffuser choked, as in the present tests. The variation of (uncorrected) Mach number during a run is within 0.001. Average flow angularity was determined by comparing force measurements made with the model erect and inverted. The implied average downwash angle was found to be up to about 0.03°.
3.6.2 Temperature variation	The temperature is controlled during the run by altering the flow of water through the cooler in the settling chamber. Temperature can be controlled to within 0.5°C. Temperature variation within the tunnel is not known.
3.6.3 Flow unsteadines	Overall turbulence level is not known but overall noise level is typically $c_{prms} = 0.004$. For further information on the noise characteristics of the wind tunnel see [4].

GENERAL TUNNEL INFORMATION (NLR)

3.1 Tunnel designation	High Speed Wind Tunnel HST [5].
3.2 Organisation running the tunnel	National Aerospace Laboratory NLR, Amsterdam, The Netherlands.
3.3 Tunnel characteristics	Closed circuit; see Fig. 9 for operating conditions.
3.4 Test section	
3.4.1 Model mounting	See Fig.5 and 6.
3.4.2 Test section dimensions	2.00 m x 1.60 m x 2.70 m (width x height x length).
3.4.3 Wall geometry	Slotted top and bottom wall; closed side walls; open area ratio 12% per wall.
3.5 Freestream conditions	
3.5.1 Reference flow condition	Total pressure: settling chamber. Static pressure: from plenum pressure with correction derived from long static pipe calibration. Static temperature: from total temperature in settling chamber and Mach number.
3.5.2 Tunnel calibration	'Long static pipe' at tunnel center and side wall pressures. Last 'long static pipe' calibration: 1980; regular checks on possible changes from side wall pressures.
3.6 Flow quality (empty tunnel)	
3.6.1 Flow uniformity	Mach number variation over model length: < .001 (at Mach=.75). Mach number variation during a run :< ± .001. Flow angularity derived from comparison of model upright and inverted tests at tunnel center; order of magnitude .2°. Variation of flow angularity over model span: not measured; estimated to be less than .2°.
3.6.2 Temperature variation	Temperature can be controlled during a run; variation during a run less than 1°C to 3°C depending on Mach and Reynolds number.
3.6.3 Flow unsteadiness	Turbulence level not measured but assumed to be very low in view of the high contraction ratio (1 : 25). Overall noise level: depending on Mach number, .5% $< c_{prms} <$ 1%.

3 GENERAL TUNNEL INFORMATION (ONERA)	
3.1 Tunnel designation	ONERA-S2MA wind tunnel (ONERA Modane Centre) [10], [11]
3.2 Organization running the tunnel	ONERA
3.3 Tunnel characteristics	
Type of tunnel	Continuous with two interchangeable test sections (1 transonic, 1 supersonic).
Indicate operating envelope	As far as the transonic test section is concerned: Mach number range: $0.25 \leq M \leq 1.35$ Total pressure: $0.3 \leq p_0 \leq 2.5$ bar The maximum total pressure depends on the Mach number. Total temperature: $285 \leq T_0 \leq 320$K
3.4 Test section	
3.4.1 Model installation	See Fig. 10.
3.4.2 Test section dimensions	1.75 m x 1.77 m x 5.40 m (width x heigth x length).
3.4.3 Wall geometry details	
Type of walls	Perforated top and bottom walls; solid side walls.
Open area ratio	6% geometric porosity (maximum).
Are wall pressures/wall displacements measured	No
Boundary layer control on walls	No
Typical wall boundary layer displacement thickness	Side wall boundary layer displacement thickness δ_1 = 14mm.
3.5 Freestream conditions	
3.5.1 Reference conditions	
Total pressure	Measured in the settling chamber.
Static pressure	Measured on the side wall, at reference pressure tap (PT 629 bis; see Fig. 10).
Static temperature	Derived from total temperature measured in the settling chamber.
3.5.2 Tunnel calibration	
How was the tunnel calibrated	By static pressure measurements along the tunnel axis using a cylinder probe (length = 6m).
Date of the last calibration	The last calibration before the present tests took place in june 1978.
3.6 Flow quality (empty tunnel)	
3.6.1 Flow uniformity	
Static pressure variation over model length and span	$\Delta M/m = \pm 3 \times 10^{-3}/m$ in x-direction ($0.7 \leq M \leq 1.2$); unknown in y-direction at the time of the F4 tests.
Mach number variation during a run	At fixed angle of attack the Mach number is kept constant at $\pm$ 0.001. During a continuous angle of attack variation, the Mach number variation depends on model size and M.
How is average flow angularity determination	By tests with model erected and inverted.

Variation of flow angularity over the model length and span	Unknown at the time of the F4 tests.
3.6.2 Temperature variation	
Can the temperature be controlled during a run	Partially, depending on the test conditions.
Variation within the tunnel	Unknown
Variation over a run	Variable, depending on the test conditions.
3.6.3 Flow unsteadiness	
Overall turbulence level	Tu ~ 0.002.
Overall noise level	$\frac{p'_{rms}}{q}$ = 0.012 at M = 0.75.

4 INSTRUMENTATION

4.1 Model postion (DRA)	
4.1.1 Geometrical angle of incidence	Model incidence derived from support angle corrected for model deflection under load as obtained by calibration.
4.1.2 Accuracy of geometrical incidence	± 0.005°
4.1 Model position (NLR)	See Fig. 6 for mounting details; model incidence derived from support angle corrected for model deflection under load as obtained by calibration. Accuracy: ± .02°.
4.1 Model postion (ONERA)	
4.1.1 How is the geometrical incidence measured	By both inclinometer in the model and model support angle corrected for model and sting deflection under aerodynamic load.
4.1.2 Accuracy of geometrical incidence	± 0.02°
4.2 Model pressure measurements	
4.2.1 Total number and disposition of pressure holes	Wing: 252 at 7 spanwise stations. Fuselage: 44 in upper and lower bottom line (see Fig.11).
4.2.2 Range and accuracy of pressure transducers	Differential transducers were used mainly ranging from 17.5 to 33 kPa and connected groupwise according to the expected pressures. Accuracy: ± .2% full scale.
4.3 Force and moment measurements (DRA)	Forces and moments were measured using a six-component internal strain gauge balance. The position of the balance is shown in Fig. 4. The ranges of the six components are as follows:

Component	Range
Axial force	670 N
Normal force	7100 N
Side force	1560 N
Pitching moment	750 Nm
Rolling moment	240 Nm
Yawing moment	240 Nm

Accuracies: Precision ± 0.05%
Bias: not determined precisely but believed to be better than ± 0.2%.

4.3 Force and moment measurements (NLR)	Task 2" extended range Component — Range Normal force — 9220 N Axial force — 930 N Pitching moment — 461 Nm Accuracy: ± .3% full scale
4.3 Force and moment measurements (ONERA)	
4.3.1 Type and location of balance	Internal 6-component strain gauge balance Φ55 n° 2
4.3.2 Indicate maximum range and accuracy of all components	Normal force N = 20000 N Axial force A = 1700 N Pitching moment M = 1700 Nm the accuracy being 0.1% full scale.
4.5 Surface flow visualizations (NLR)	Wing upper and lower surface. Acenaphtene to optimize transition strips. Oil flow pictures during and after a run. Data available on photographs.
4.5 Surface flow visualizations(ONERA)	
4.5.1 Measurement technique applied	a) Acenapthene for transition location. b) Oil flow and c) Coloured liquid for wall streamlines.
4.5.2 On which surfaces is the flow visualized	a) Transition location on the right wing. b) Wall streamlines on the left wing.
4.5.3 In what form are data available	Photographs
4.7 Tunnel wall measurements (DRA)	
4.7.1 Types of measurements	Four static pressures were measured close to the peak decrement in pressure on the roof and two on the floor. These holes were, respectively, 152mm upstream and downstream of the balance centre-line which is 11.6mm downstream of the moment reference point of the model.
4.7 Tunnel wall measurements(ONERA)	
4.7.1 Type of measurements	None, except static pressure reference measurements
4.7.2 Location and number of pressure holes	See Fig. 10.

5 TEST MATRIX AND CONDITIONS

5.1 Detailed test matrix	
5.1.1 Number of selected test cases	
5.1.2 Number of configurations	2 ; wing/body (W/B) and body alone (B)
5.1.3 Refer to table	Table 1: Force measurements
Test case number	see Table 1
Configuration	wing/body body alone
Mach number	0.6, 0.75, 0.80
Reynolds number	$3.0 \cdot 10^6$
Model attitude	$-4° < \alpha < 10°$, $\beta = 0°$
Type of measurements	force measurements (Fig. 12).
Refer to table	Table 2:Pressure measurements, M-sweep
Test case number	see Table 2
Configuration	wing/body
Mach number	M = 0.6, 0.7, 0.75, 0.76, 0.77, 0.78, 0.79, 0.80, 0.81, 0.82
Reynolds number	$3.0 \cdot 10^6$
Model attitude	$c_L = 0.5$
Type of measurements	pressure distribution on wing and body.

Refer to table	Table 3: Pressure measurements, c_L-sweep
Test case number	see Table 3
Configuration	wing/body
Mach number	0.75
Reynolds number	$3.0 \cdot 10^6$
Model attitude	c_L = 0.3, 0.4, 0.5, 0.6
Type of measurements	pressure distribution on wing and body (Fig. 13).

5.2 Model/tunnel relations

5.2.1 Maximum blockage

DRA-8ft x 8ft	
NLR-HST	0.0081
ONERA-S2MA	0.0084

5.2.2 Model span/tunnel width

DRA-8ft x 8ft	0.480
NLR-HST	0.586
ONERA-S2MA	

5.2.3 Wing area/tunnel cross-section

DRA-8ft x 8ft	0.0244
NLR-HST	0.0454
ONERA-S2 MA	0.0469

5.2.6 Adiabatic wall temperatures (DRA)	Reached by ensuring minimal excursion of model temperature between wind on and wind off conditions.
5.2.6 Adiabatic wall temperatures(ONERA)	yes, in principle

5.3 Transition details

5.3.1 Free or fixed transition	fixed
5.3.3 Details of fixed transition	see Fig. 14. sparsely distributed carborundum grains, strips about 2 mm wide; optimized by each wind tunnel.
DRA-8ft x 8ft	upper surface 220 K, lower surface 180 K transition verified by special DRA routine including drag measurements
NLR-HST	upper surface 180 K, lower surface 240 K transition verified with acenaphtene
ONERA-S2MA	upper surface 220 K, lower surface 240 K transition verified with acenaphtene

6 DATA

6.1 Availability of data

6.1.1 Organisation	Deutsche Forschungsanstalt für Luft- und Raumfahrt (DLR) Institut für Entwurfsaerodynamik
6.1.2 Responsible Person	Dr.-Ing. G. Redeker DLR Postfach 3267 38022 Braunschweig Fed. Rep. Germany Tel.: 49 531 295 2430; Fax: 49 531 295 2320

6.1.3 Availability	Data are freely available.
6.2 Suitability of data for CFD validation	
6.2.1 Are data suitable for 'in-tunnel' calculations?	No; but uncorrected data of DRA can be used for in-tunnel calculations.
6.2.2 Corrections	Data are corrected to „free-air" conditions.
6.3 Type and form in which data are available	
6.3.1 Type and form	Tables of wing and body geometry Tables of force coefficients and pressure coefficients
6.3.2 Data carrier	3.5" floppy disk (geometry and aerodynamic data).
6.3.3 Extent of geometry data	142 kBytes
6.3.4 Extent of aerodynamic test data	213 kBytes
6.4 Corrections applied to data (DRA)	
6.4.1 Lift interference and blockage corections	Corrections to angle of incidence and drag coefficient for lift interference obtained using linear theory [7, 8] and the measured lift coefficient. The model is small for the test section and the data are considered to be globally correctable for lift interference. Corrections to Mach number and free-stream static and dynamic pressures were obtained using a method [9] that is standard for the 8ft x 8ft Tunnel. The method is of the model-representation type with the model and wake displacement effects allowed for by an axial distribution of point sources and sinks. The solid walls are represented by a suitable doubly infinite array of images. The ratio of the blockage velocity increment on the tunnel centre line at the moment reference point to the total (direct plus blockage) velocity increment on the tunnel walls at the pressure measuring points is then calculated. The ratio is then used in conjuntion with the measured pressure increments relative to empty-tunnel conditions to give the blockage correction. No corrections have been applied to drag for blockage buoyancy, but see below.
6.4.4 Sting corrections	Apart from correcting base pressure to free-stream static pressure, no corrections have been applied for sting interference. However, tests were made with the body alone as well as with the wing-body. By differencing wing-body and body alone data, it is possible to obtain notional 'wing alone' data largely free of sting interference and blockage buoyancy effects.
6.4.5 Aeroelastic deformation	See 6.4.5 Corrections applied to data (NLR).
6.4 Corrections applied to data (NLR)	
6.4.1 Lift interference and blockage corrections	For the size of the model data are considered to be interference free (this is based on a number of comparisons between the HST and other wind tunnels).
6.4.2 Sting and support corrections	Static pressures are corrected for the upstream support influence using the empty tunnel center line pressure distribution (with the model support present) as measured with a long static pipe.
6.4.4 Other corrections	Buoyancy drag derived from static pressure variation as measured with long static pipe and support present.
6.4.5 Aeroelastic deformation	A theoretical estimate has been made of the wing deformation under load (see Fig. 15) for the 'design' condition at $Re=3 \times 10^6$. This deformation is not included in the geometrical wing data.

6.4 Corrections applied to data (ONERA)

6.4.1 Lift interference and blockage corrections	
Are data considered globally correctable	yes
Type of correction method applied	analytical [12].
Specify what data are actually corrected and indicate order of magnitude	The following corrections, for example, have been applied at $M = 0.75$, $c_L = 0.5$ Mach number: $\Delta M = -0.0001$ Drag coefficient: $\Delta c_D = -0.00059$
6.4.4 Sting and support corrections	
Correction method	Computation of the flowfield induced by the support
Magnitude and typical variation of support induced pressure field	The magnitude of support induced pressure field results, at $M = 0.75$, $c_L = 0.5$, in a correction of the drag coefficient $\Delta c_{DS} = +0.00192$
6.4.5 Aeroelastic deformation	
How was deformation determined	by NLR computation
Typical order of magnitude	wing tip twist angle $\Delta\alpha = -0.43°$ (Fig. 15)
6.4.6 Other corrections	Empty test section flow buoyancy leading to a correction of the drag coefficient $\Delta c_{Db} = +0.00071$.

7 DATA ACCURACY AND REPEATABILITY ASSESSMENT (DRA)

7.1 Accuracy

7.1.1 Freestream conditions	Incidence	±0.01°
	Mach number	±0.001
7.1.2 Measured data Forces and Moments	Lift coefficient	±0.004
	Drag coefficient	±0.0004
	Pitching moment coefficient	±0.001
Pressure	Pressure coefficient	±0.002

7.2 Repeat measurements	Tests of the model in the erect and inverted positions have been made. The discrepancies between the two sets of data for the drag are well within the band $\Delta c_D = \pm 0.0001$.
7.4 Other tests made	The same model was tested in the ONERA-S2MA and NLR-HST wind tunnels.

7 DATA ACCURACY AND REPEATABILITY ASSESSMENT (NLR)

7.1 Accuracy estimates

7.1.1 Free stream conditions	Δ Mach $< \pm 0.002$ $\Delta\alpha < \pm 0.02°$
7.1.2 Measured data	$\Delta c_L < \pm 0.005$ $\Delta c_D < \pm 0.0005$ $\Delta c_M < \pm 0.002$ $\Delta c_p < \pm 0.005$ (0.01 in pressure peaks)
7.2 Repeat measurements	no repeat measurements made
7.3 Redundant measurements	Forces have been measured with and without pressure wiring

	present. Static load checks ('α-sweeps') have been made with model in inverted position showing agreement within measurement accuracy. Measured wing and body pressures have been integrated to be compared with measured overall forces.
7.4 Other tests made	The same model was tested in the ONERA- S2MA and in the DRA-8ft x 8ft wind tunnels.

7 DATA ACCURACY AND REPEATABILITY ASSESSMENT (ONERA)

7.1 Accuracy estimates	
7.1.1 Free stream conditions	
Mach number	$\Delta M = \pm\ 0.001$
Model incidence	$\Delta\alpha = \pm\ 0.02°$
7.1.2 Measured data	
Forces and moments	$\Delta c_L = \pm\ 0.006$ $\Delta c_D = \pm\ 0.0004$ $\Delta c_M = \pm\ 0.0014$
Pressure coefficients	$\Delta c_p = \pm\ 0.01$
7.2 Repeat measurements	
7.2.1 Type and number of repeat measurements within one test campaign	Reduced number of total force and moment measurements as well as wing pressure distributions.
7.3 Redundant measurements	
7.3.2 Checks made on internal consistency of the data	Shock wave and separation locations by pressure distribution and surface flow visualisations. Buffet onset determination by lift curve, pitching moment curve, tangential force curve, rms-value curve of wing root strain gauge, wing tip accelerometer.
7.4 Other tests on same (nominal) geometry	
7.4.1 Has the same (identical) model been measured in another wind tunnel?	The same model was tested in the NLR-HST and in the DRA (former RAE) 8ft x 8ft wind tunnels as a GARTEUR exercise.

8 REFERENCES

G. Redeker; R. Müller: A comparison of Experimental Results for the Transonic Flow around the DFVLR-F4 Wing Body Configuration.
GARTEUR/TP-018
DLR-IB 129 - 83/21 (1983).

[2] K.G. Winter; L. Gaudet:
Turbulent boundary-layer studies at high Reynolds number. ARC R&M 3712, 1970

[3] D. Isaacs:
Calibration of the RAE Bedford 8ft x 8ft Wind Tunnel at Subsonic Speeds, Including a Discussion of the Correction to the Measured Pressure Distribution to Allow for the Direct and Blockage Effects due to the Calibration Probe. ARC R&M 2777, 1969.

[4] J. Whitfield; N.S. Dougherty Jr.:
A Survey of Transition Research at AEDC. Paper 25-1, AGARD-CP-224, 'Laminar-Turbulent Transition', Oct. 1971.

[5] User's guide to the 1.60 x 2.00 m^2 High Speed Wind Tunnel HST of the National Aerospace Laboratory NLR.

[6] R.H.C.M. Hirdes:
Test results of wind-tunnel measurements on the DFVLR-F4 wing in the NLR high speed wind tunnel HST. NLR TR 83131 L, 1983.

[7] H.C. Garner:
Subsonic wind tunnel wall corrections. AGARDograph 109, 1966.

[8] W.E.A. Acum:
Corrections for symmetrical and tapered wings in rectangular wind tunnels. ARC R&M 2777.

[9] B. Goethert:
Windkanalkorrekturen bei hohen Unterschallgeschwindigkeiten unter besonderer Berücksichtigung des geschlossenen Kreiskanals.
Deutsche Luftfahrtforschung Forschungsbericht 1216, 1940 (translated as NACA Tech Memo 1300).

[10] M. Pierre; G.Fasso:
The aerodynamic test center of Modane-Avrieux. ONERA - TN no 166E, 1972.

[11] M. Pierre, G. Fasso:
Exploitation du centre d'essais aerothermodynamique de Modane-Avrieux. ONERA - TN no 181, 1971

[12] X. Vaucheret:
Améliorations des calculs des effects de parois dans les souffleries industrielles de l'ONERA. AGARD - CP - 335, 1982.

9 LIST OF SYMBOLS

Coordinate system of wing/body configuration (see Fig. 1).	x,y,z
coordinate system of wing (see Fig. 1)	
half span in x-y system	
half span in x*-y* system	$s^* = b^*/2$
wing ref. area	S
leading edge sweep angle	φ_{LE}
quarter chord line sweep angle	φ_{25}
local wing chord	c
aerodynamic mean chord	
spanwise coordinate non-dimensional	$\eta = \frac{y}{s} = \frac{y^*}{s^*}$
aspect ratio of wing	$\Lambda = b^2/S$
taper ratio	λ
fuselage diameter	D
fuselage length	
Mach number	M
angle of attack	α
lift coefficient	$c_L = L/(q_\infty \times S)$
pitching moment coefficient with ref. to N_{25} (see Fig. 1).	$c_M = M/(q_\infty \times S \times \tilde{c})$
drag coefficient	$c_D = D/(q_\infty \times S)$
normal force coefficient	$c_N = N/(q_\infty \times S)$
tangential force coefficient	$c_T = T/(q_\infty \times S)$
freestream dynamic pressure	q_∞
freestream static pressure	p_∞
local surface pressure	p
pressure coefficient	$c_p = (p-p_\infty)/q_\infty$
Reynolds number based on aerodynamic mean chord	Re

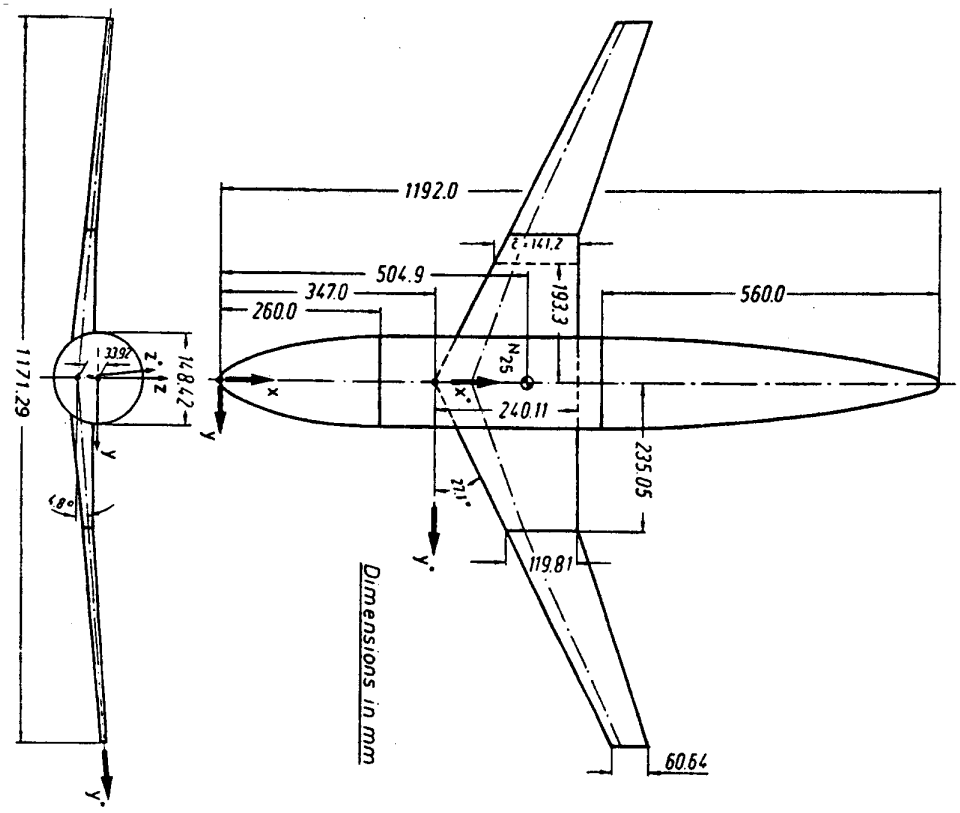

Fig. 1 General arrangement of the DLR-F4 wind tunnel model

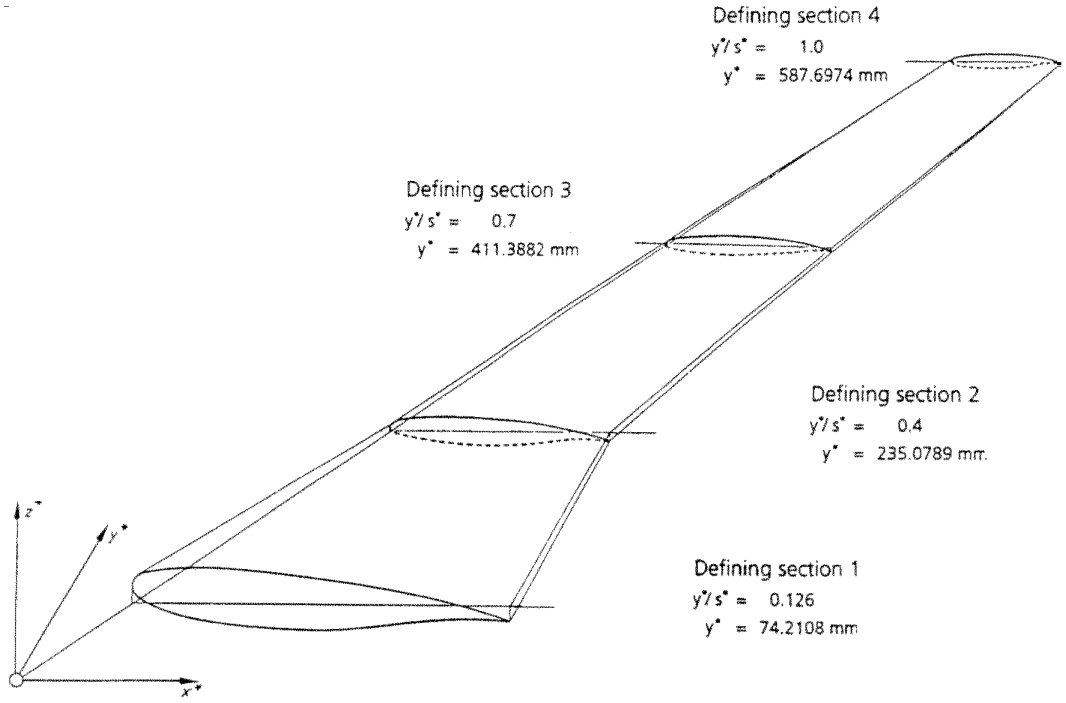

Fig. 2 Definition of the wing

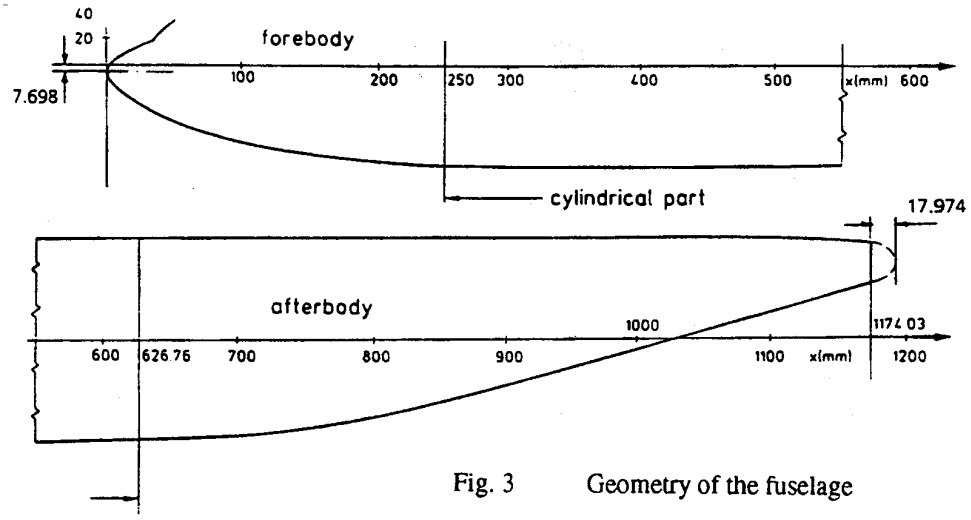

Fig. 3 Geometry of the fuselage

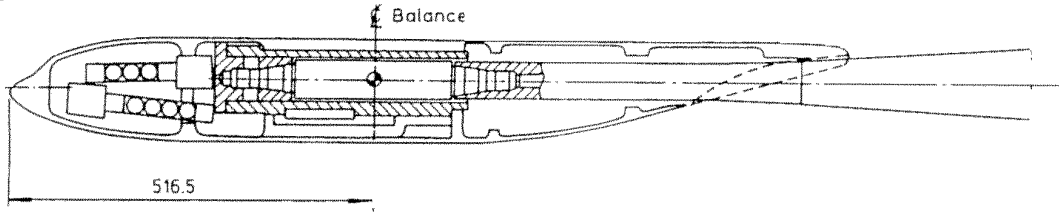

Fig. 4 Arrangement for mounting model in the DRA 8ftx8ft wind tunnel

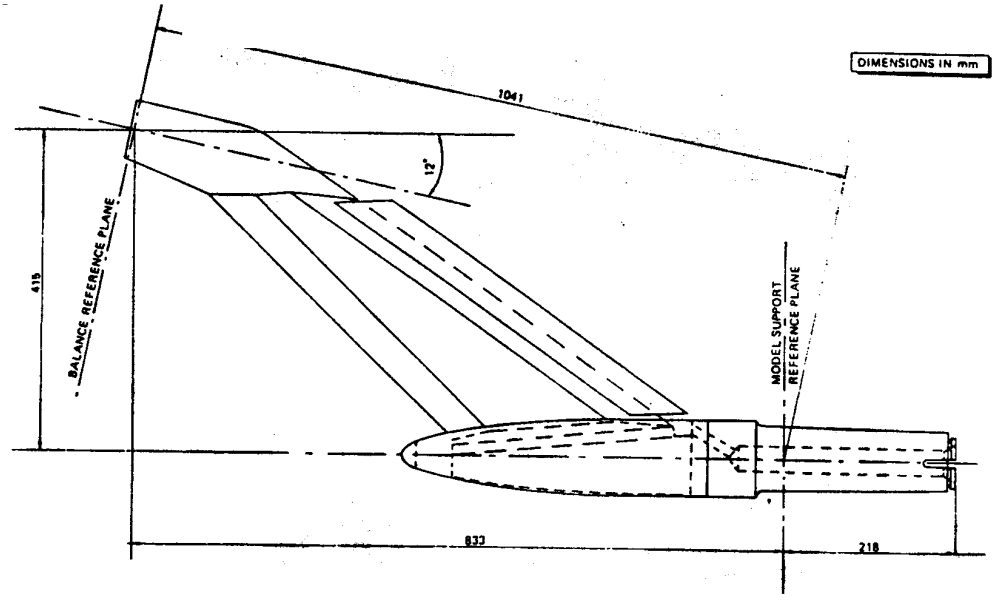

Fig. 5 Dimensions of NLR z-sting Nr. 002

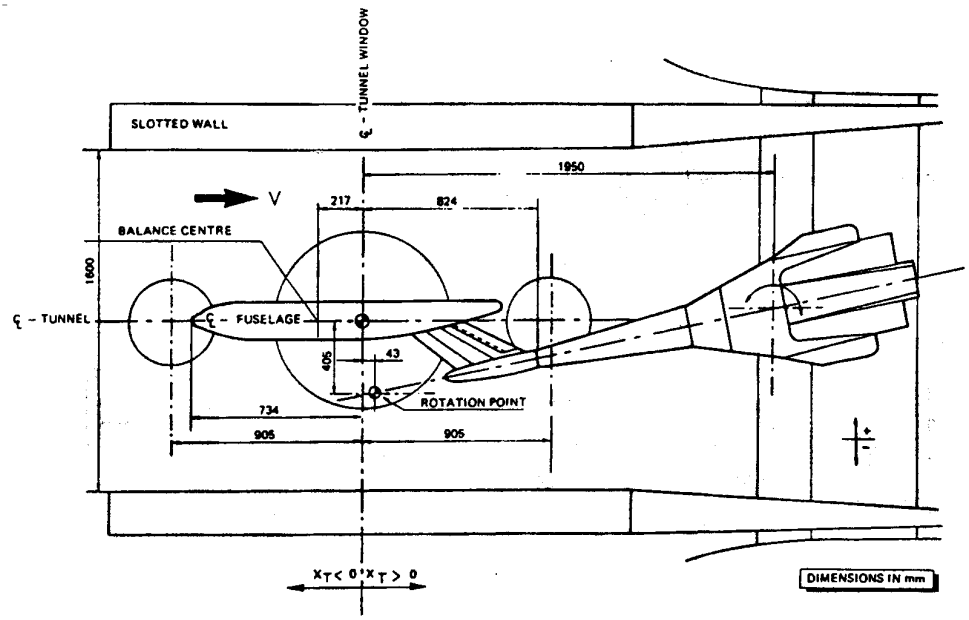

Fig. 6 Position of DLR-F4 model in the HST test-section

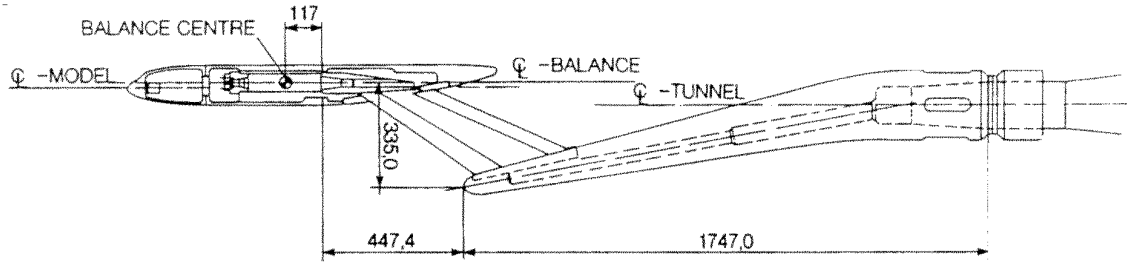

Fig. 7 ONERA z-sting arrangement

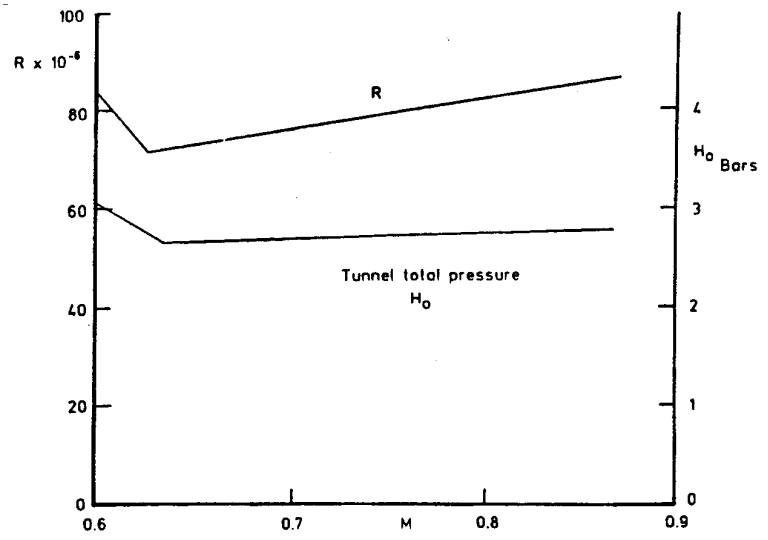

Fig. 8 DRA 8ftx8ft wind tunnel capability at high subsonic speeds

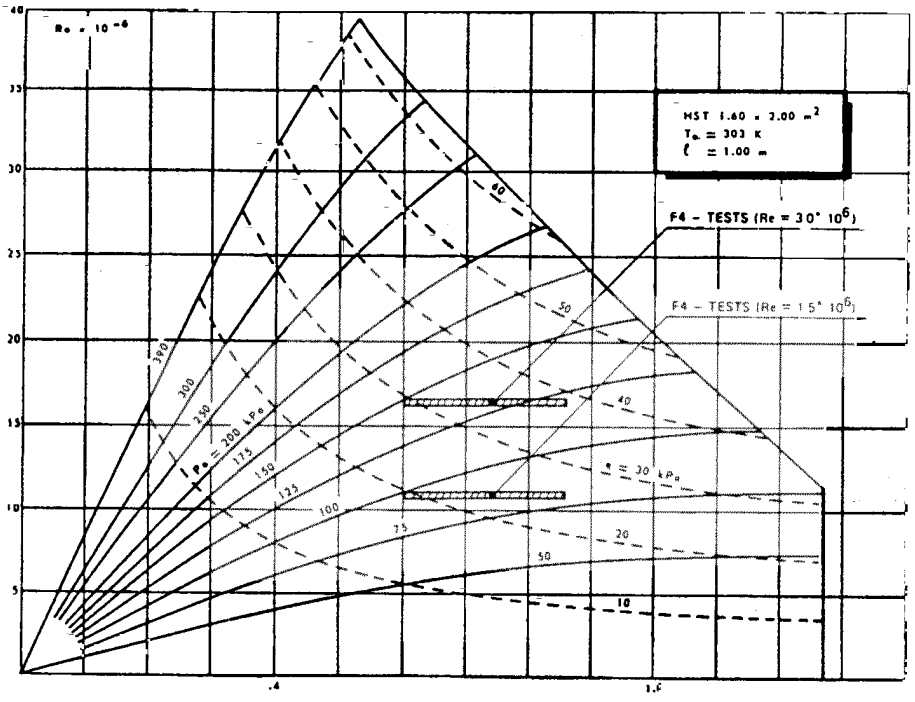

Fig. 9 Reynolds number as function of Mach number in empty test section of NLR-HST

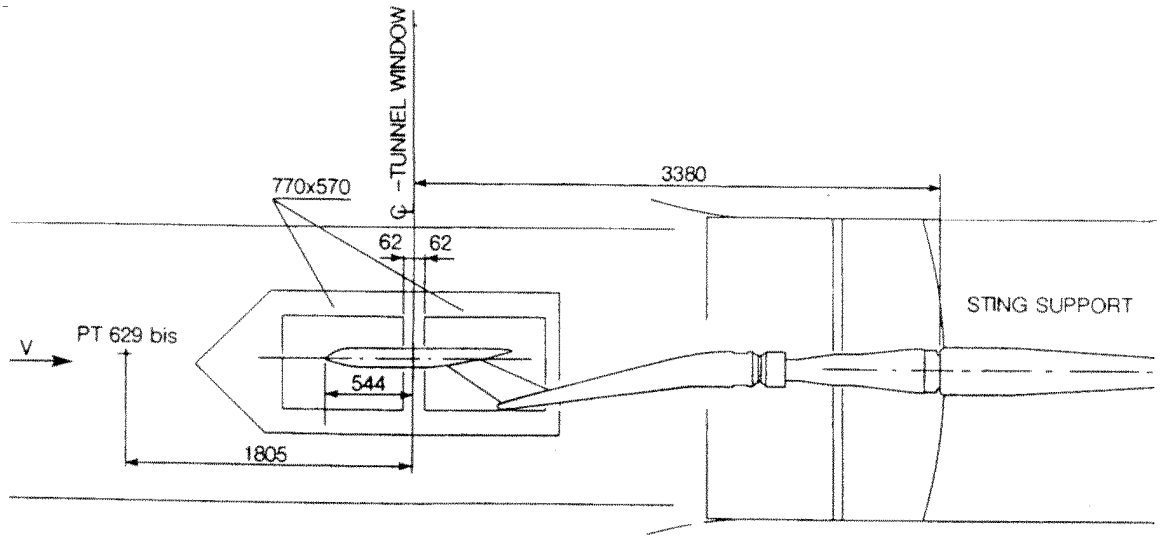

Fig. 10 S2MA-transonic test section with test set-up of DLR-F4 model

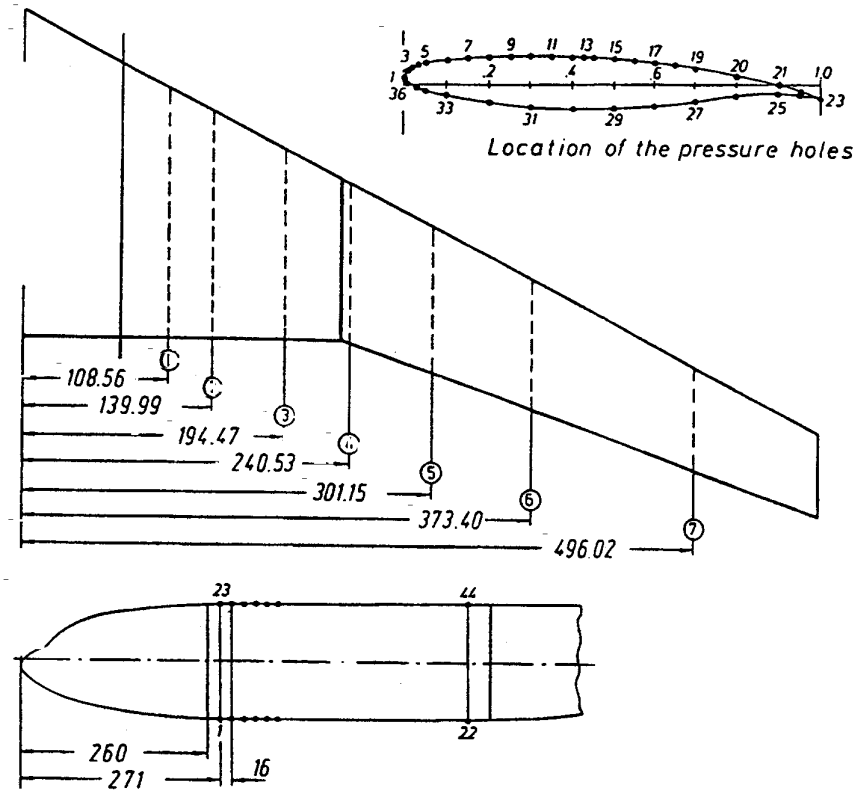

Fig. 11 Positition of pressure holes on wing and fuselage

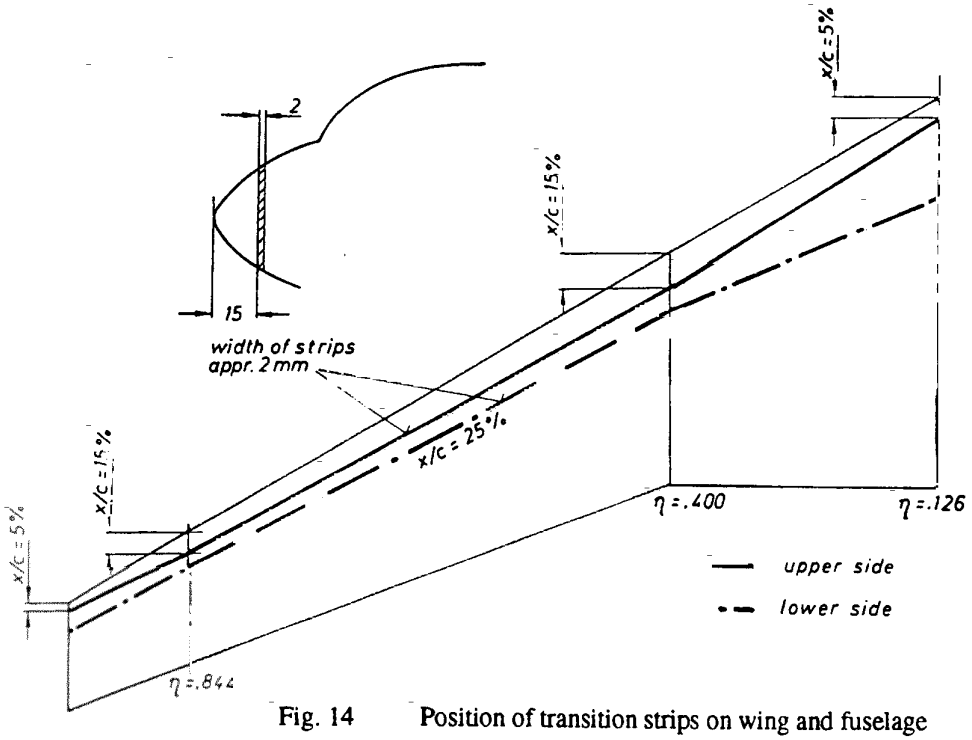

Fig. 14 Position of transition strips on wing and fuselage

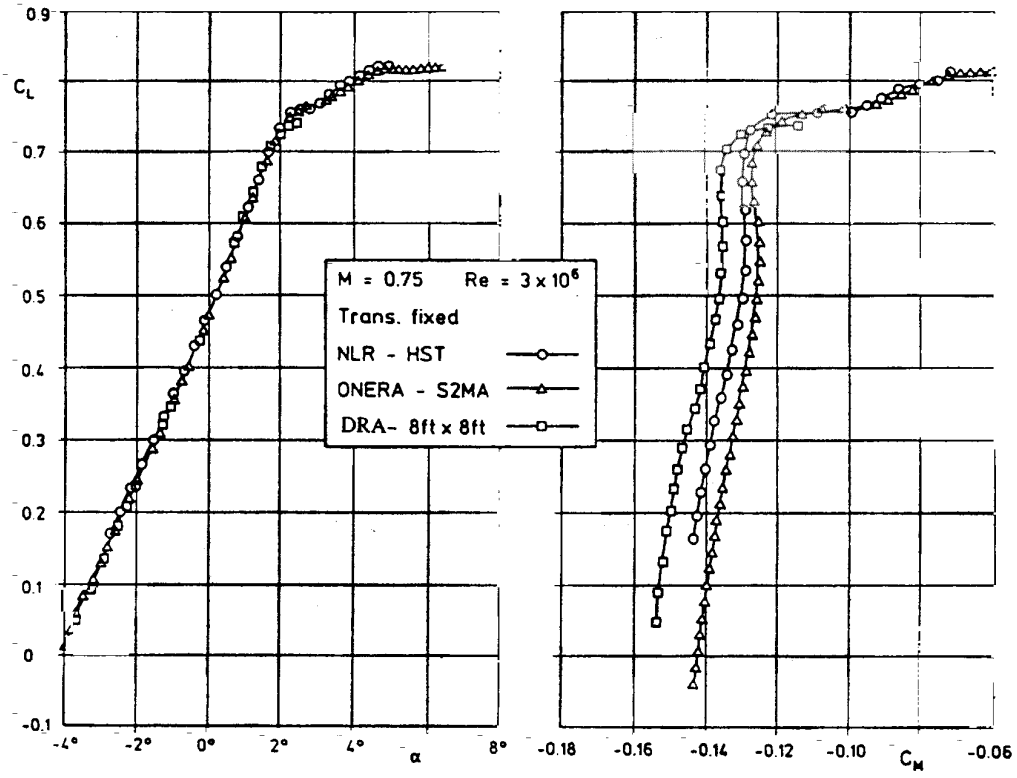

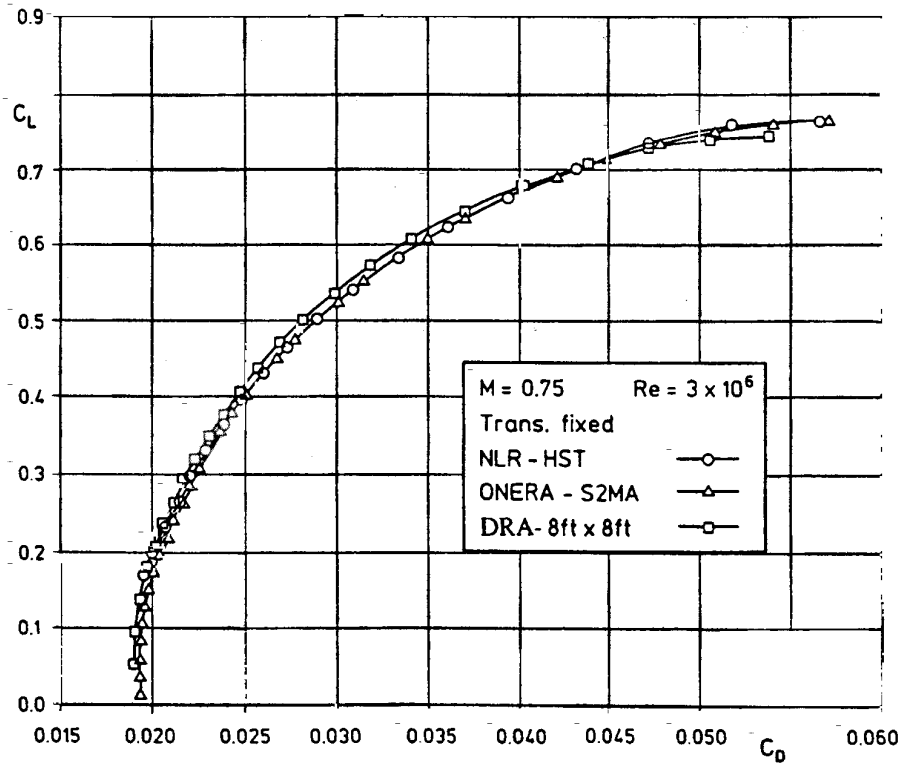

Fig. 12 Comparison of force and pitching moment coefficients of DLR-F4 model

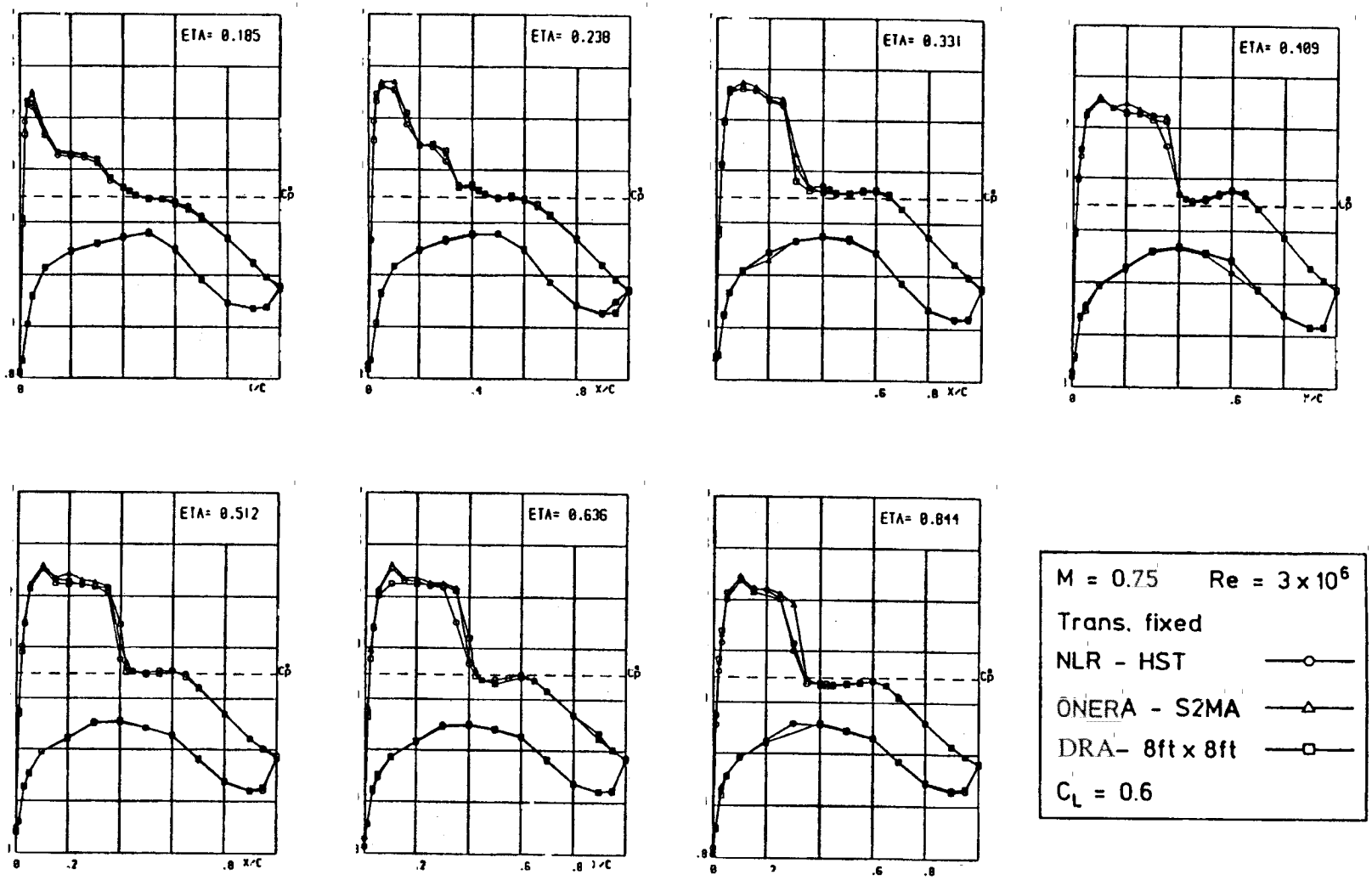

Fig. Comp ng pr distri utions of LR model

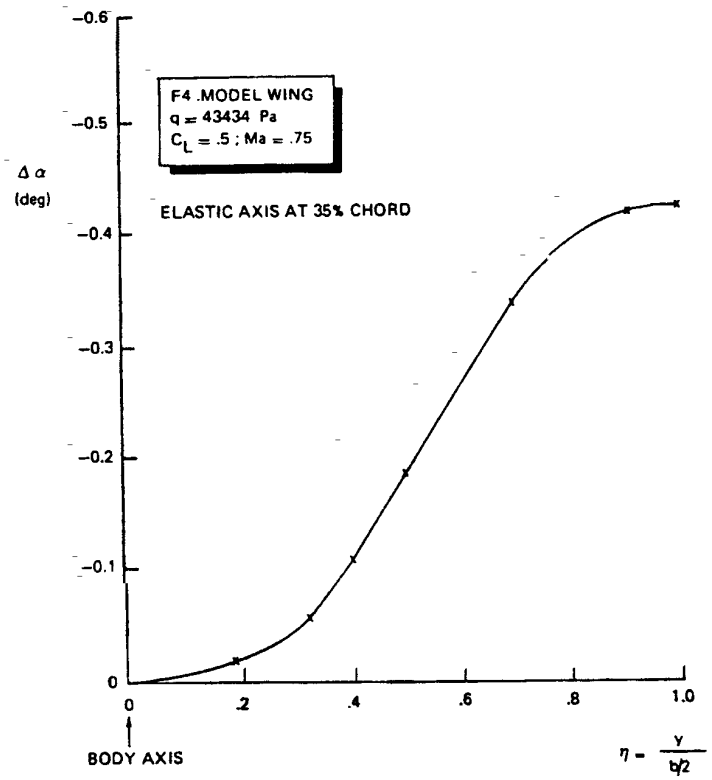

Fig. 15 Calculated wing deformation of DLR-F4 model

	M = 0.60		M = 0.75		M = 0.80	
	W/B	B	W/B	B	W/B	B
NLR - HST	1.1.1.1	1.1.2.1	1.1.1.2	1.1.2.2	1.1.1.3	1.1.2.3
ONERA-S2MA	1.2.1.1	1.2.2.1	1.2.1.2	1.2.2.2	1.2.1.3	1.2.2.3
DRA - 8ft x 8ft	1.3.1.1	1.3.2.1	1.3.1.2	1.3.2.2	1.3.1.3	1.3.2.3

Table 1: Force measurements, α-sweep at various Mach numbers, Re = $3.0 \cdot 10^6$

	M = 0.60	M = 0.70	M = 0.75	M = 0.76	M = 0.77
	W/B	W/B	W/B	W/B	W/B
NLR - HST	2.1.1.1	2.1.1.2	2.1.1.3	----------	2.1.1.5
ONERA-S2MA	2.2.1.1	2.2.1.2	2.2.1.3	2.2.1.4	2.2.1.5
DRA - 8ft x 8ft	2.3.1.1	2.3.1.2	2.3.1.3	----------	2.3.1.5

	M = 0.78	M = 0.79	M = 0.80	M = 0.81	M = 0.82
	W/B	W/B	W/B	W/B	W/B
NLR - HST	2.1.1.6	2.1.1.7	2.1.1.8	2.1.1.9	2.1.1.10
ONERA-S2MA	2.2.1.6	2.2.1.7	2.2.1.8	2.2.1.9	2.2.1.10
DRA - 8ft x 8ft	2.3.1.6	2.3.1.7	2.3.1.8	2.3.1.9	2.3.1.10

Table 2: Pressure distribution, Mach number - sweep Re = $3.0 \cdot 10^6$, $c_L = 0.50$

	$c_L = 0.3$	$c_L = 0.4$	$c_L = 0.5$	$c_L = 0.6$
	W/B	W/B	W/B	W/B
NLR - HST	3.1.1.1	3.1.1.2	2.1.1.3	3.1.1.3
ONERA-S2MA	3.2.1.1	3.2.1.2	2.2.1.3	3.2.1.3
DRA - 8ft x 8ft	3.3.1.1	3.3.1.2	2.3.1.3	3.3.1.3

Table 3: Pressure distribution, c_L - sweep Re = $3.0 \cdot 10^6$, M = 0.75

Explanation of the notation of Table 1 to Table 3.

In order to identify tables with the aerodynamic data, they are numbered with a four digit figure w.x.y.z. The meaning of the digits w,x,y,z is described below.

1. digit describes the kind of aerodynamica data
   - w = 1 force and moment data
   - w = 2 pressure distribution M-sweep
   - w = 3 pressure distribution c_L-sweep

2. digit indicates the wind tunnel, where the data has been achieved
   - x = 1 NLR-HST
   - x = 2 ONERA-S2MA
   - x = 3 DRA-8ft x 8ft

3. digit determines the configuration
   - y = 1 wing/body
   - y = 2 body

4. digit is a running number to identify the various cases in one group.

REPORT DOCUMENTATION PAGE

1. Recipient's Reference	2. Originator's Reference	3. Further Reference	4. Security Classification of Document
	AGARD-AR-303 Volume II	ISBN 92-836-1003-2	UNCLASSIFIED

5. Originator Advisory Group for Aerospace Research and Development
North Atlantic Treaty Organization
7 rue Ancelle, 92200 Neuilly-sur-Seine, France

6. Title
A Selection of Experimental Test Cases for the Validation of CFD Codes

7. Presented at

8. Author(s)/Editor(s)	9. Date
Multiple	August 1994
10. Author's/Editor's Address	**11. Pages**
Multiple	596

12. Distribution Statement There are no restrictions on the distribution of this document. Information about the availability of this and other AGARD unclassified publications is given on the back cover.

13. Keywords/Descriptors

Computational fluid dynamics
Aerodynamic configurations
Aircraft
Missiles
Wind tunnel tests
Data bases
Validity

14. Abstract

This report presents the results of a study by Working Group 14 of the AGARD Fluid Dynamics Panel. This group was formed to establish an accessible, detailed experimental data base for the validation of Computational Fluid Dynamics (CFD) codes.

The thirty nine test cases that are documented cover the subsonic, transonic, and supersonic flow regimes and five classes of geometries. Included in the five classes of geometries are: Two Dimensional Airfoils; Three Dimensional Wings, designed for predominantly attached flow conditions; Slender Bodies, typical of missile type configurations; Delta Wings, characterized by a conical type of vortex flow; and Complex Configurations, either in a geometrical sense or because of complicated flow interactions.

The report is presented in two volumes. Volume I provides a review of the theoretical and experimental requirements, a general introduction and summary of the test cases, and recommendations for the future. Volume II contains detailed information on the test cases. The relevant data of all test cases has been compiled on floppy disks, which can be obtained through National Centers.